Pergamon

Int. J. Solids Structures Vol. 33, No. 30, pp. 4481–4494, 1996

0020–7683/96 $15.00 + .00

0020–7683(95)00278–2

EXACT SOLUTION OF ORTHOTROPIC CYLINDRICAL SHELL WITH PIEZOELECTRIC LAYERS UNDER CYLINDRICAL BENDING

CHANG-QING CHEN, YA-PENG SHEN and XIAO-MING WANG
Department of Engineering Mechanics, Xi'an Jiaotong University, Xi'an Shaanxi Province, 710049 P.R. China

(*Received* 9 *June* 1995; *in revised form* 30 *October* 1995)

Abstract—An exact elasticity solution for an orthotropic cylindrical shell with piezoelectric layers is obtained in this paper. The stress and displacement distributions are presented. The influence of the piezoelectric layers on the mechanical behavior of structures is studied. Both the direct piezoelectric effect and the converse piezoelectrical effect of the piezoelectric material are investigated. Results presented in this paper can be used to study various approximate shell theories used in the numerical simulations of piezoelectric structures. Copyright © 1996 Elsevier Science Ltd

1. INTRODUCTION

The use of distributed sensors and actuators integrated with structures has become the subject of focus in recent years, and these structures have been termed intelligent or smart structures. There are two characteristics of piezoelectrical materials which permit them to be used as sensors and actuators. One is their direct piezoelectric effect which implies that the materials induce electric charge or electric potential when they are subjected to external mechanical deformations. Conversely, they are deformed if some electric charge or electric potential is imposed on them.

Structures with distributed piezoelectric sensors and actuators have been investigated by many researchers. Crawley and de Luis (1987) developed analytical models for surface-bonded and embedded piezoelectric actuators of an intelligent beam. Wang and Rogers (1991) employed the classical laminated plate theory (CLPT) to obtain an analytical solution of a laminate plate with spatially distributed actuators through Heaviside and Delta functions. Crawley and Lazarus (1991) investigated a cantilevered plate with piezoelectric sensors and actuators by virtue of the consistent plate model. The Rayleigh–Ritz technique has been used, and both analytical and experimental results are obtained. Ray *et al.* (1993a, 1993b) obtained the three-dimensional exact solution for laminated plates with piezoelectric layers. In addition, a number of papers have been published using the finite element method (FEM). Tzou (1991) and his coworkers (1991) proposed a general shell theory for FEM analysis. Chandrashekhara and Agarwal (1993) and Hwang (1993) presented plate FEM using first order shear plate theory (other references can be found in their papers).

However, the exact elasticity solution of a laminated shell with piezoelectric layers which can be used in numerical analyses to assess approximate results is still unavailable. In this paper, an exact elasticity solution for a simply-supported orthotropic shell strip with piezoelectric layers under cylindrical bending is obtained.

2. FUNDAMENTAL FORMULATIONS AND SOLUTION

2.1. *Governing equations and boundary conditions*

The laminated infinitely long shell considered here consists of two piezoelectric layers as its top and bottom layers and a cylindrically orthotropic graphite/epoxy composite substrate with fibre parallel or perpendicular to the circumferential direction, illustrated in

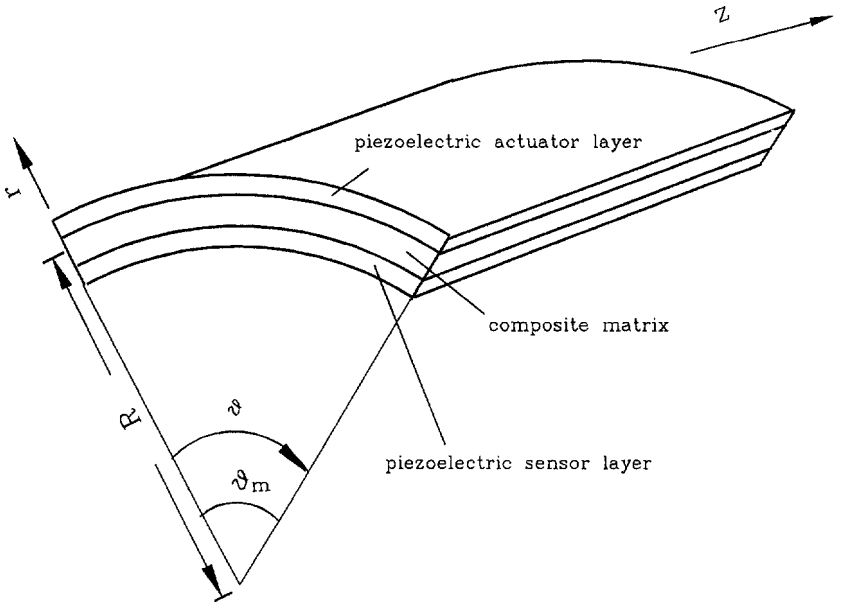

Fig. 1. The configuration of the laminated cylindrical shell.

Fig. 1. A normal traction is applied on the outer surface with the inner surface free from traction. The top piezoelectric layer is used as an actuator while the bottom one acts as sensors.

The cylindrical polar coordinate system (r, θ, and z) is used in this paper where r, θ, and z refer to the radial, circumferential and axial directions, respectively. u_r, u_θ, and u_z are the corresponding displacements. The equilibrium equations and the charge equilibrium equation of the piezoelectric medium under cylindrical bending have the forms:

$$\begin{aligned} \sigma_{r,r}+\tau_{r\theta,\theta}/r+(\sigma_r-\sigma_\theta)/r &= 0 \\ \tau_{r\theta,r}+\sigma_{\theta,\theta}/r+2\tau_{r\theta}/r &= 0 \end{aligned} \tag{1}$$

and

$$D_r+rD_{r,r}+D_{\theta,\theta}=0 \tag{2}$$

where subscript comma denotes differentiation and D_r and D_θ are the electric displacements in the r and θ directions.

The relations of the strain–displacement and electric field $\{E\}$-electric potential ψ in the cylindrical coordinate system are

$$\begin{aligned} \varepsilon_r &= u_{r,r} \\ \varepsilon_\theta &= (u_{\theta,\theta}+u_r)/r; \\ \gamma_{r\theta} &= (u_{r,\theta}-u_\theta)/r+u_{\theta,r} \end{aligned} \tag{3}$$

and

$$\begin{aligned} E_r &= -\psi_{,r} \\ E_\theta &= -\psi_{,\theta}/r. \end{aligned} \tag{4}$$

Although the piezoelectric material considered in Section 3 is elastically isotropic and uniaxially polarized, i.e., a voltage applied across its face (the radial direction) results in a circumferential strain due to the piezoelectric stress coefficient e_{31}, it is treated here as a cylindrically orthotropic material for convenience. Other piezoelectric stress coefficients are

considered to be absent. The linear constitutive equations coupling the elastic and electric fields in the piezoelectric medium are given by

$$\begin{Bmatrix} \sigma_r \\ \sigma_\theta \\ \tau_{r\theta} \end{Bmatrix} = \begin{bmatrix} C_{11} & C_{12} & 0 \\ C_{12} & C_{22} & 0 \\ 0 & 0 & C_{66} \end{bmatrix} \begin{Bmatrix} \varepsilon_r \\ \varepsilon_\theta \\ \gamma_{r\theta} \end{Bmatrix} - \begin{bmatrix} e_{33} & 0 \\ e_{31} & 0 \\ 0 & e_{15} \end{bmatrix} \begin{Bmatrix} E_r \\ E_\theta \end{Bmatrix} \tag{5}$$

$$\begin{Bmatrix} D_r \\ D_\theta \end{Bmatrix} = \begin{bmatrix} e_{33} & e_{31} & 0 \\ 0 & 0 & e_{15} \end{bmatrix} \begin{Bmatrix} \varepsilon_r \\ \varepsilon_\theta \\ \tau_{r\theta} \end{Bmatrix} + \begin{bmatrix} \varepsilon_{rr} & 0 \\ 0 & \varepsilon_{\theta\theta} \end{bmatrix} \begin{Bmatrix} E_r \\ E_\theta \end{Bmatrix} \tag{6}$$

where $[e]$ is the piezoelectric stress coefficient (actually, only e_{31} of the piezoelectric stress coefficients in eqn (5) and (6) is non-zero for the piezoelectric material considered in this paper and $[\varepsilon]$ is the piezoelectric coefficient).

The boundary conditions are

(1) Simply-supported edge boundary conditions for each layer

$$u_r = \sigma_\theta = \tau_{\theta z} = \psi = 0 \quad (\theta = 0, \theta_m). \tag{7}$$

(2) Interface continuity conditions for σ_r, $\tau_{r\theta}$, u_r, and u_θ.

(3) For the piezoelectric actuator layer on the outer surface

$$\begin{aligned} \sigma_r &= q_0 \sin(p\theta) \\ \tau_{r\theta} &= 0 \\ \psi &= V_1 \sin(p\theta) \end{aligned} \tag{8}$$

on the interface $\psi = 0$ and those of continuity conditions,

(4) For the piezoelectric sensor layer on the inner surface

$$\sigma_r = \tau_{r\theta} = D_r = 0 \tag{9}$$

on the interface $\psi = 0$ and those of continuity conditions,

where $p = m\pi/\theta_m$, m is an integer and V_1 and q_0 are prescribed values.

2.2. *Solution*

The displacement functions and the electric potential function satisfying the simply-supported edge boundary conditions are given by

$$\begin{aligned} u_r &= \varphi_r(r) \sin(p\theta) \\ u_\theta &= \varphi_\theta(r) \cos(p\theta) \\ \psi &= \Psi(r) \sin(p\theta). \end{aligned} \tag{10}$$

Substituting eqn (10) into (3) and (4) and then into (5) and (6) yields the governing differential equations of the piezoelectric layers from eqn (1) and (2),

$$\begin{aligned} &C_{11}(\varphi_r'' + \varphi_r'/r) - (C_{22} + p^2 C_{66})\varphi_r/r^2 \\ &\quad - p(C_{66} + C_{12})\varphi_\theta'/r + p(C_{66} + C_{22})\varphi_\theta/r^2 - e_{31}\Psi'/r = 0 \end{aligned} \tag{11}$$

$$p(C_{66}+C_{12})\varphi_r'/r+p(C_{22}+C_{66})\varphi_r/r^2$$
$$+C_{66}(\varphi_\theta''+\varphi_\theta'/r)-(p^2C_{22}+C_{66})\varphi_\theta/r^2+pe_{31}\Psi'/r=0 \quad (12)$$

$$e_{31}\varphi_r'/r-pe_{31}\varphi_\theta'/r-\varepsilon_{rr}(\Psi''+\Psi'/r)+p^2\varepsilon_{\theta\theta}\Psi/r^2=0 \quad (13)$$

where superscript $'$ refers to the differentiation corresponding to r. Equations (11) and (12) are also the governing equations for the orthotropic composite substrate when the variables related to electric displacements and electric potential are dropped. Notice that eqns (11), (12), and (13) are Euler equations. After assuming the solution of them in form of

$$\begin{Bmatrix}\varphi_r\\ \varphi_\theta\\ \Psi\end{Bmatrix}=\begin{Bmatrix}A_r\\ A_\theta\\ A_\Psi\end{Bmatrix}r^s \quad (14)$$

we get the auxiliary equation

$$As^6+Bs^4+Cs^2+D=0 \quad (15)$$

where

$$A=-C_{11}C_{66}\varepsilon_{rr}$$
$$B=p^2C_{11}C_{66}\varepsilon_{\theta\theta}+[C_{11}(p^2C_{22}+C_{66})+C_{66}(C_{22}+p^2C_{66})]\varepsilon_{rr}$$
$$+C_{66}e_{31}^2-p^2(C_{66}+C_{12})^2\varepsilon_{rr}+p^2C_{11}e_{31}^2$$
$$C=-(C_{22}+p^2C_{66})(p^2C_{22}+C_{66})\varepsilon_{rr}-p^2[C_{11}(p^2C_{22}+C_{66})+C_{66}$$
$$(C_{22}+p^2C_{66})]\varepsilon_{\theta\theta}+2p^2(C_{66}+C_{22})e_{31}^2-(p^2C_{22}+C_{66})e_{31}^2$$
$$+p^4(C_{66}+C_{12})^2\varepsilon_{\theta\theta}+p^2(C_{22}+C_{66})^2\varepsilon_{rr}-p^2(C_{22}+p^2C_{66})e_{31}^2$$
$$D=p^2(p^2C_{22}+C_{66})(C_{22}+p^2C_{66})\varepsilon_{\theta\theta}-p^4(C_{22}+C_{66})^2\varepsilon_{\theta\theta}.$$

Equation (15) can be transformed into standard cubic equation as

$$\alpha^3+g\alpha+f=0 \quad (16)$$

where

$$\alpha=s^2+\frac{B}{3A}$$
$$g=-\frac{B^2-3AC}{3A^2}$$
$$f=\frac{2B^3-9ABC+27A^2D}{27A^3}.$$

Equation (16) has three distinct real roots, three real roots with at least two of them being equal, or a real root in conjunction with two complex roots depending on the following expression

$$Q=\frac{f^3}{4}+\frac{g^3}{27} \quad (17)$$

is negative, zero, or positive, respectively.

For the case considered in this paper Q of eqn (17) is negative. Hence, there exist three distinct real roots given by

$$\alpha_1 = 2\sqrt{\frac{-g}{3}}\cos\left(\frac{\beta}{3}\right)$$

$$\alpha_2 = -2\sqrt{\frac{-g}{3}}\cos\left(\frac{\beta+\pi}{3}\right)$$

$$\alpha_3 = -2\sqrt{\frac{-g}{3}}\cos\left(\frac{\beta-\pi}{3}\right) \tag{18}$$

where β satisfies

$$\cos\beta = -\frac{f}{2\sqrt{-\left(\frac{g}{3}\right)^3}}.$$

Therefore, the roots of eqn (15) are also distinct (actually, all the roots are real for the piezoelectric material considered here). For a distinct root s_j ($j = 1, 6$), eqn (14) can be expressed as

$$\begin{Bmatrix} \varphi_r \\ \varphi_\theta \\ \Psi \end{Bmatrix} = \begin{Bmatrix} 1 \\ H_\theta(s_j) \\ H_\Psi(s_j) \end{Bmatrix} A_j r^{s_j} \tag{19}$$

where A_j is an arbitrary constant, and

$$H_\theta(s_j) = -\{p[(C_{66}+C_{12})s_j + C_{66}+C_{22}](-\varepsilon_{rr}s_j^2 + p^2\varepsilon_{\theta\theta}) - pe_{31}^2 s_j^2\}/\Delta$$

$$H_\psi(s_j) = -\{[C_{66}s_j^2 - (p^2C_{22}+C_{66})]e_{31}s_j + p^2 e_{31}s_j[(C_{66}+C_{12})s_j + C_{66}+C_{22}]\}/\Delta$$

$$\Delta = [C_{66}s_j^2 - (p^2C_{22}+C_{66})](-\varepsilon_{rr}s_j^2 + p^2\varepsilon_{\theta\theta}) + p^2 e_3^2 s_j^2.$$

The general solution of eqns (11), (12), and (13) is thus obtained

$$\begin{Bmatrix} \varphi_r \\ \varphi_\theta \\ \Psi \end{Bmatrix} = \begin{bmatrix} r^{s_1} & r^{s_2} & \dots & r^{s_6} \\ H_\theta(s_1)r^{s_1} & H_\theta(s_2)r^{s_2} & \dots & H_\theta(s_6)r^{s_6} \\ H_\Psi(s_1)r^{s_1} & H_\Psi(s_2)r^{s_2} & \dots & H_\Psi(s_6)r^{s_6} \end{bmatrix} \begin{Bmatrix} A_1 \\ A_2 \\ A_6 \end{Bmatrix}. \tag{20}$$

The elasticity solution of the orthotropic composite substrate has been obtained by Ren (1987) through a stress function. In this paper, it is got by using displacement functions similar to those of Bhaskar and Varadan's (1993). When the electric variables are dropped eqns (11) and (12) are also the governing equations of the orthotropic composite substrate while the elastic constants are those of the corresponding layer of the substrate. The solutions are assumed to be

$$\begin{Bmatrix}\varphi_r^{(k)}\\ \varphi_\theta^{(k)}\end{Bmatrix}=\begin{Bmatrix}B_r^{(k)}\\ B_\theta^{(k)}\end{Bmatrix}r^t \tag{21}$$

where superscript k refers to the kth layer of the composite substrate. Through a similar procedure, we get the characteristic equation of the composite layer

$$at^4+bt^2+c=0 \tag{22}$$

where

$$a=C_{11}^{(k)}C_{66}^{(k)}$$
$$b=-C_{66}^{(k)}(C_{22}^{(k)}+p^2C_{66}^{(k)})-C_{11}^{(k)}(p^2C_{22}^{(k)}+C_{66}^{(k)})+p^2(C_{66}^{(k)}+C_{12}^{(k)})^2$$
$$c=(C_{22}^{(k)}+p^2C_{66}^{(k)})(p^2C_{22}^{(k)}+C_{66}^{(k)})-p^2(C_{22}^{(k)}+C_{66}^{(k)})^2.$$

All the roots of eqn (22) are distinct positive real for any composite layer considered in this paper. Therefore, the general solution of the kth layer of the substrate has a similar form as eqn (20)

$$\begin{Bmatrix}\varphi_r^{(k)}\\ \varphi_\theta^{(k)}\end{Bmatrix}=\begin{bmatrix}H_r^{(k)}(t_1)r^{t_1} & \dots & H_r^{(k)}(t_4)r^{t_1}\\ r^{t_1} & \dots & r^{t_4}\end{bmatrix}\begin{Bmatrix}B_1^{(k)}\\ B_4^{(k)}\end{Bmatrix} \tag{23}$$

where

$$H_r^{(k)}(t_j)=\frac{p[(C_{66}^{(k)}+C_{12}^{(k)})t_j-(C_{(66)}^{(k)}+C_{22}^{(k)})]}{C_{11}^{(k)}t_j^2-(C_{22}^{(k)}+p^2C_{66}^{(k)})}.$$

All the unknown constants of eqn (20) and (23) can be determined by satisfying the boundary conditions.

3. NUMERICAL EXAMPLES

The piezoelectric material considered here is elastically isotropic and uniaxially polarized. The material properties are

$$E=2\,\text{GPa}\quad \nu=0.29\quad e_{31}=0.046(\text{C/m}^2)$$
$$\varepsilon_{11}=\varepsilon_{22}=\varepsilon_{rr}=\varepsilon_{\theta\theta}=0.106\text{E-}9(\text{F/m}). \tag{24}$$

The material properties of the graphite/epoxy composite are those used by Ren (1987)

$$E_L=172\,\text{GPa(25E6 psi)}\quad E_T=6.9\,\text{GPa(1E6 psi)}$$
$$G_{LT}=3.4\,\text{GPa(0.5E6 psi)}\quad G_{TT}=1.4\,\text{GPa(0.2E6 psi)}$$
$$\nu_{LT}=\nu_{TT}=0.25 \tag{25}$$

where subscript L denotes the fibre direction and T refers to the transverse direction.

Two cases of the composite substrate are considered as the numerical examples

(1) Single-layered substrate with fibre parallel to the θ direction.
(2) Three-layered substrate with fibre of the center layer and of top and bottom layers oriented in the z direction and the θ direction, respectively, each layer being of equal thickness.

In both cases, $\theta_m=\pi/3$ and $m=1$. Moreover, all variables are non-dimensionalized as

Table 1. Maximum displacement and stress

	Present			Ren (1987)		
S	$u_r^*(0,\theta_m/2)$	$\sigma_\theta^*(\mp\frac{1}{2},\theta_m/2)$	$\tau_{r\theta}^*(0,0)$	$u_r^*(0,\theta_m/2)$	$\sigma_\theta^*(\mp\frac{1}{2},\theta_m/2)$	$\tau_{r\theta}^*(0,0)$
Case 1						
		−2.455			−2.455	
2	0.997	1.907	0.555	0.999	1.907	0.555
		−0.890			−0.890	
10	0.115	0.807	0.579	0.115	0.807	0.579
		−0.758			−0.758	
100	0.0755	0.751	0.565	0.0755	0.751	0.565
Case 2						
		−3.647			−3.467	
2	1.436	2.463	0.394	1.436	2.463	0.394
		−0.995			−0.995	
10	0.144	0.897	0.525	0.144	0.897	0.525
		−0.787			−0.786	
100	0.0786	0.779	0.523	0.0787	0.781	0.523

$$\sigma_r^* = \frac{\sigma_r}{q_0} \quad \sigma_\theta^* = \frac{\sigma_\theta}{q_0 S^2} \quad \tau_{r\theta}^* = \frac{\tau_{r\theta}}{q_0 S}$$

$$u_r^* = \frac{10 E_T u_r}{q_0 H_c S^4} \quad u_\theta^* = \frac{100 E_T u_\theta}{q_0 H_c S^4}$$

$$S = R/H_c \quad \zeta = z/H_c \quad \beta = H_c/H_p \tag{26}$$

where R is the radius of the centerface of the substrate, H_c and H_p are thicknesses of the composite substrate and the piezoelectric layer and $\zeta = 0$ refers to the centerface of the substrate. In all problems, $R = 1$ and $q_0 = 1$ for simplicity.

When the piezoelectric layers are dropped, the results obtained in this paper are compared with those of Ren (1987) in Table 1. Very good agreement between them can be seen. Additionally, the present results have been found that they satisfy all the boundary conditions very well.

Figure 2 illustrates the influence of the piezoelectric layers on the mechanical properties of structures for Case 1 at $S = 10$ when no external voltage is applied on the actuator where superscript $'$ implies that variables are obtained when the piezoelectric layers are dropped. From it we can see that the piezoelectric layers have less effect on the inplane shear stress

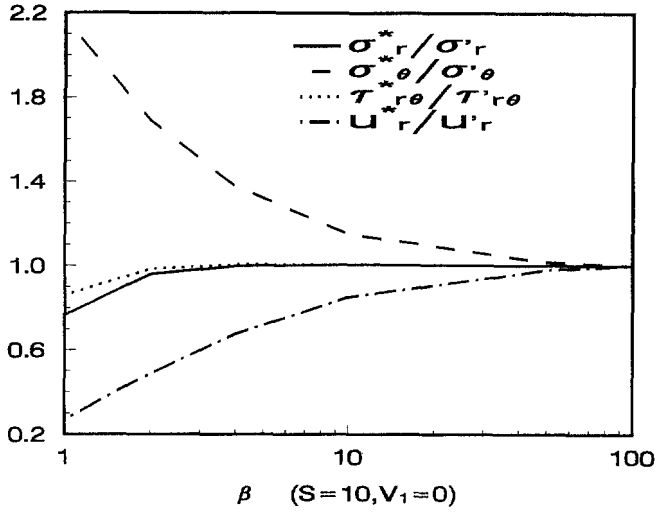

Fig. 2. Influence of the mechanical properties of piezoelectric layers on the structure for Case 1 and $S = 10$, $V_1 = 0$.

Table 2. Sensed electric potential on the inner surface of the sensor (Unit: mV)

	$\psi(-0.51, \theta_m/2)$ (Case 1)		$\psi(-0.51, \theta_m/2)$ (Case 2)	
S	$V_1 = 0$	$V_1 = 100$ (V)	$V_1 = 0$	$V_1 = 100$ (V)
2	0.133	−0.0555	0.188	−0.0677
4	0.139	−0.0679	0.186	−0.0544
10	0.228	−0.00734	0.256	0.0428
50	0.980	0.738	1.019	0.819
100	1.934	1.694	2.007	1.808
500	9.586	9.347	9.939	9.741

Table 3. Induced transverse and in-plane displacements

	Case 1				Case 2			
	$V_1 = 0$		$V_1 = 100$		$V_1 = 0$		$V_1 = 100$	
S	$u_r^*(0, \theta_m/2)$	$u_\theta^*(0, 0)$	$u_r^*(0, \theta_m/2)$	$u_\theta^*(0, 0)$	$u_r^*(0, \theta_m/2)$	$u_\theta^*(0, 0)$	$u_r^*(0, \theta_m/2)$	$u_\theta^*(0, 0)$
2	0.981	3.380	−0.405	−1.274	1.440	5.294	−0.519	−1.248
4	0.306	1.030	−0.164	−0.387	0.459	1.549	−0.163	−0.159
10	0.112	0.374	−0.0340	−0.0610	0.144	0.480	−0.0227	−0.0105
50	0.0754	0.251	0.0481	0.163	0.0808	0.269	0.0518	0.176
100	0.0740	0.247	0.0604	0.202	0.0785	0.262	0.0641	0.215

and the transverse normal stress than on the inplane normal stress and the deflection. Although their effects can be neglected when β approaches 100 in this case, there is no general conclusion in which situation the mechanical properties of the piezoelectric material are negligible. In all the following analyses, β is chosen to be 100 if there is no special indication. Therefore, $\zeta = \pm 0.51$ means the outer and inner surfaces of the shell.

The results of the direct piezoelectric effect of the sensor is shown in Table 2, and those of the converse piezoelectric effect of the actuator are presented in Table 3. Figures 3–6 illustrate the displacement and the stress distributions across the thickness with and without applied electric potential on the actuator. From these figures it can be seen that the linear variation distribution assumption of the inplane displacement and normal stress across the thickness for thin to moderate thick shells is reasonable. They also show that the transverse displacement is almost independent of r even when the radium to thickness ratio S reaches 4. When the applied electric voltage is 100 volt, the induced strain of the piezoelectric actuator layer can change the stress and displacement distributions of the structure significantly. The maximum transverse and inplane stresses occur on the interface between the substrate and the actuator layer. Figures 7–9 show the electric potential distributions of the sensor and the actuator layers across the thickness with and without applied voltage. Linearly varied voltage is found in them, which can be adopted in approximate theories.

4. CONCLUSION

An exact solution for an orthotropic cylindrical shell with piezoelectric layers under cylindrical bending is obtained. The stress and displacement distributions are presented. The results of sensed voltage and induced deformation due to the direct and the converse piezoelectric effects are shown in tabular form which can be used to assess approximate results. The results obtained here have shown that the assumptions of the linear variation of inplane displacement and normal stress and the electric potential in the piezoelectric layers are reasonable.

Acknowledgement—The support of this work from the Doctoral Education Foundation of China and the National Natural Science Foundation of China is greatly appreciated.

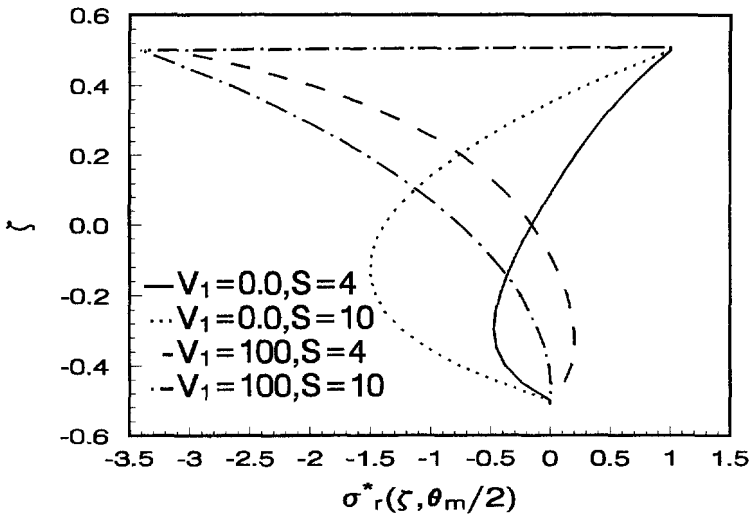

(a)

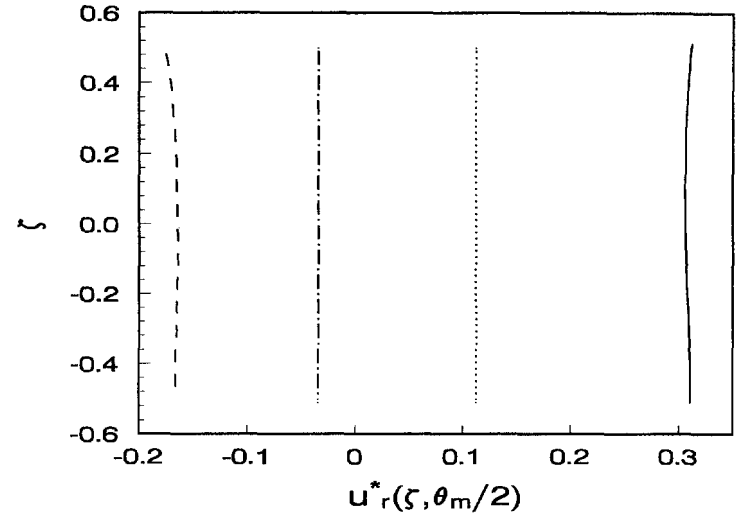

(b)

Fig. 3. The transverse displacement and distribution of Case 1 with and without applied voltage: (a) transverse normal stress σ_r^*; (b) transverse displacement u_r^*.

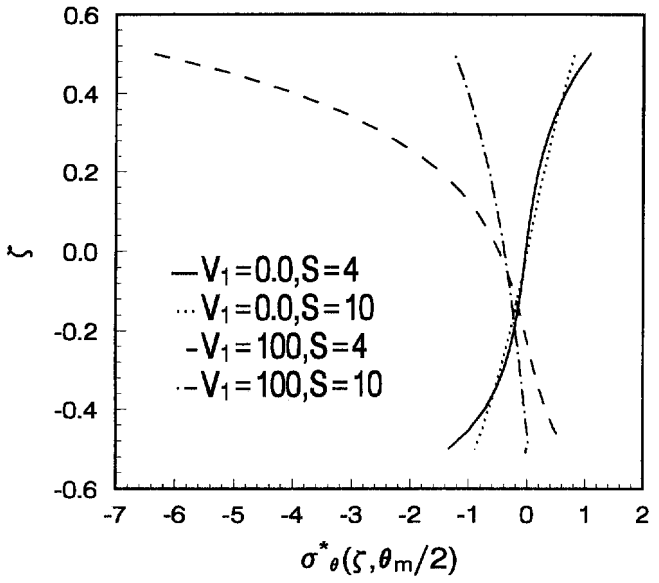

(a)

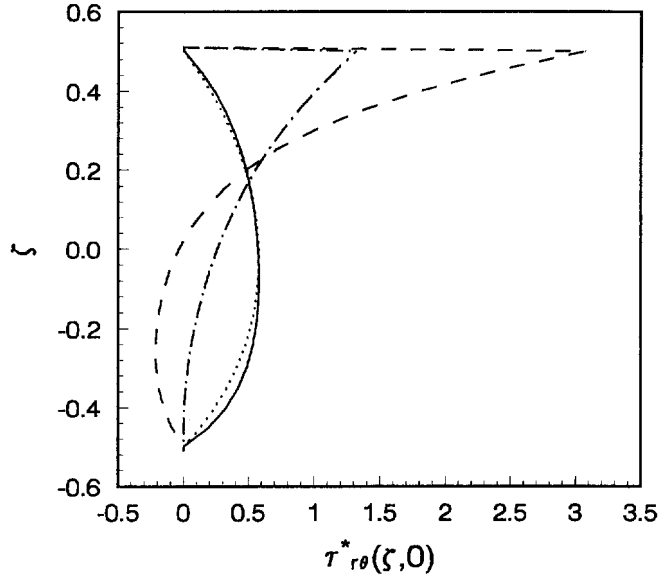

(b)

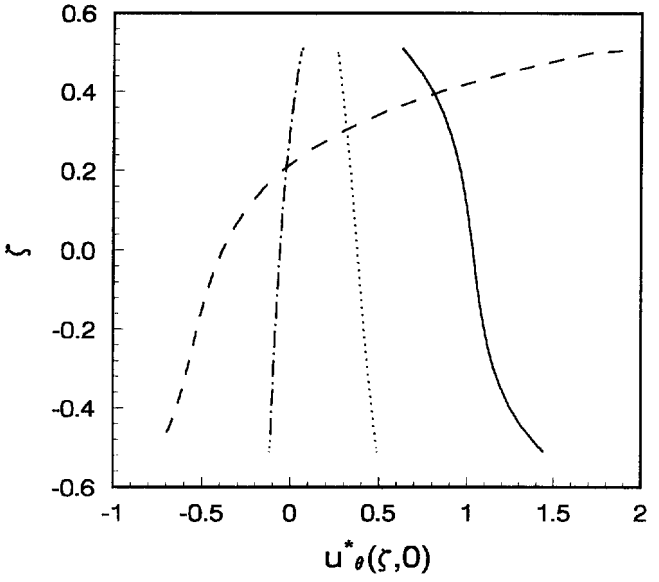

(c)

Fig. 4. The inplane displacement and stress distribution of Case 1 with and without applied voltage: (a) inplane normal stress σ_θ^*; (b) inplane shearing stress $\tau_{r\theta}^*$; (c) inplane displacement u_θ^*.

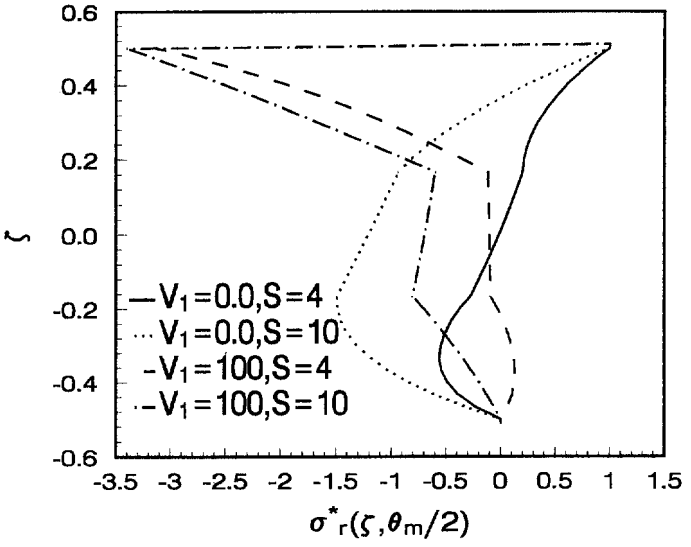

(a)

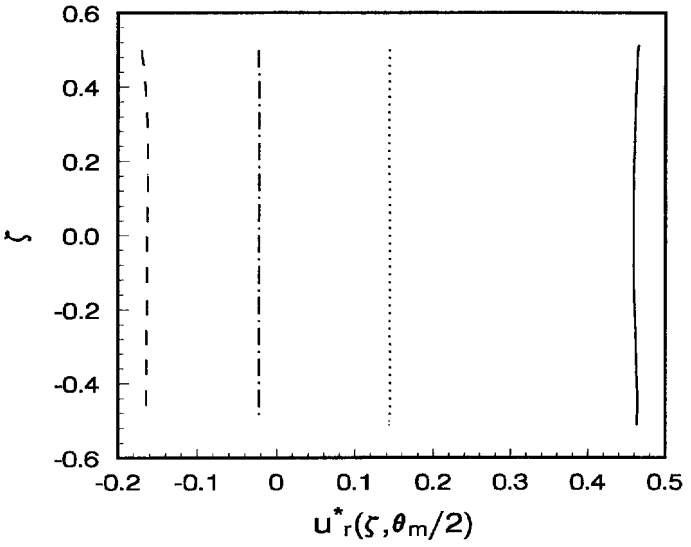

(b)

Fig. 5. The transverse displacement and stress distribution of Case 2 with and without applied voltage: (a) transverse normal stress σ_r^*; (b) transverse displacement u_r^*.

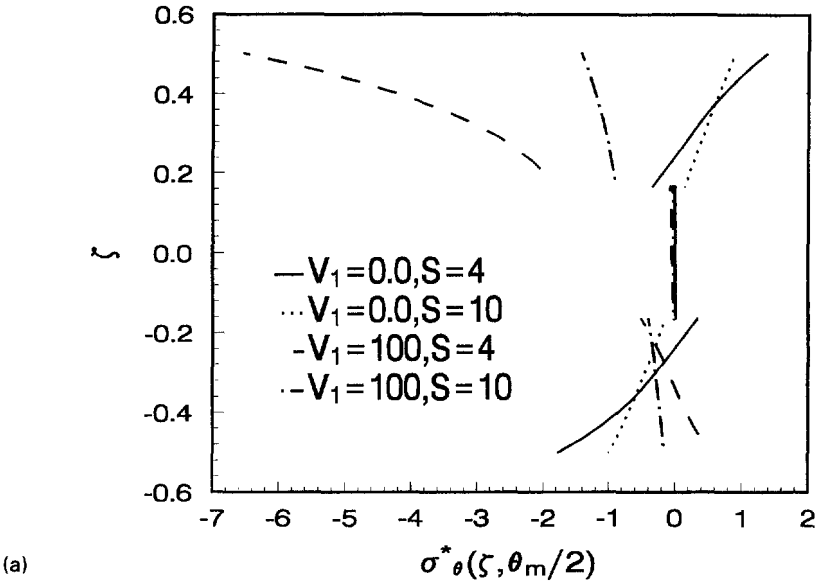

(a)

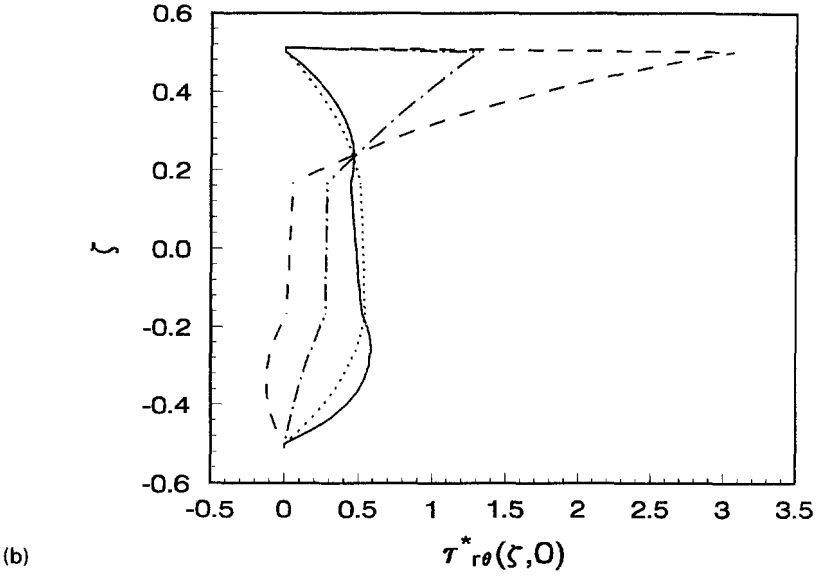

(b)

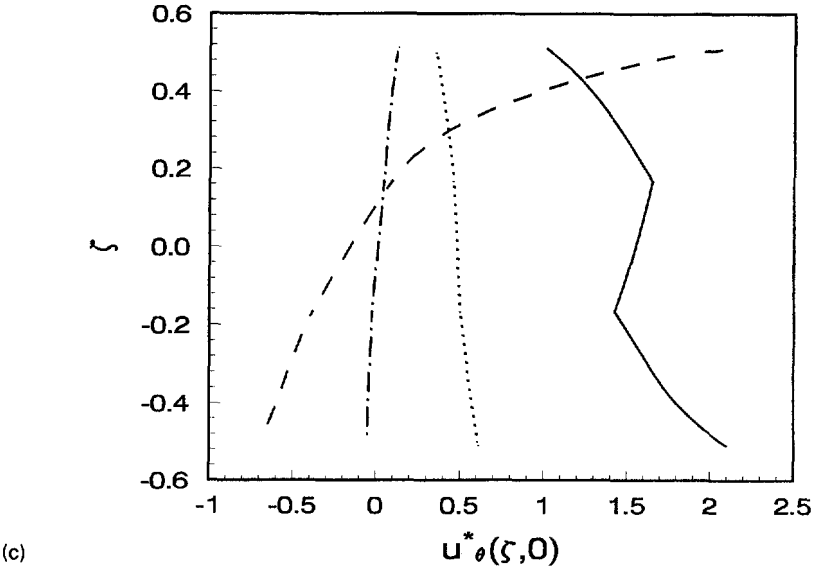

(c)

Fig. 6. The inplane displacement and stress distribution of Case 2 with and without applied voltage: (a) inplane normal stress σ_θ^*; (b) inplane shearing stress $\tau_{r\varphi}^*$; (c) inplane displacement u_θ^*.

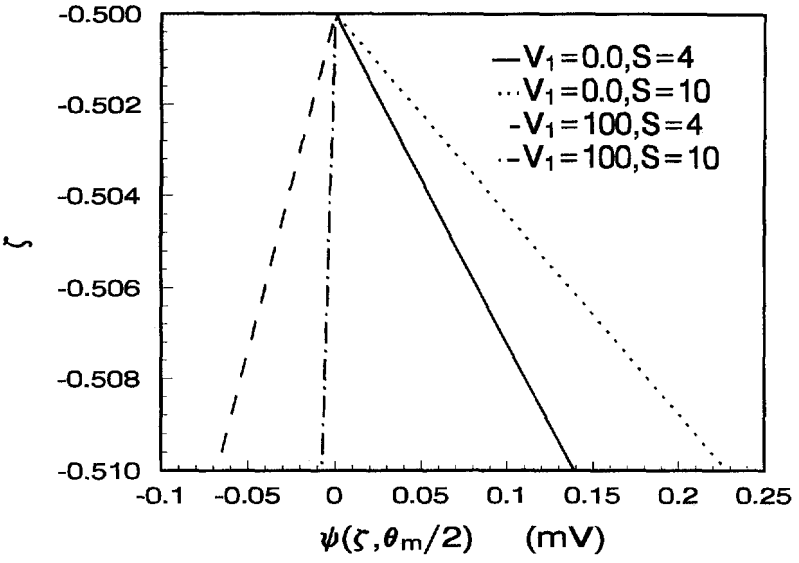

Fig. 7. The electric potential distribution in the sensor layer for Case 1 with $V_1 = 0$ and $V_1 = 100$ V.

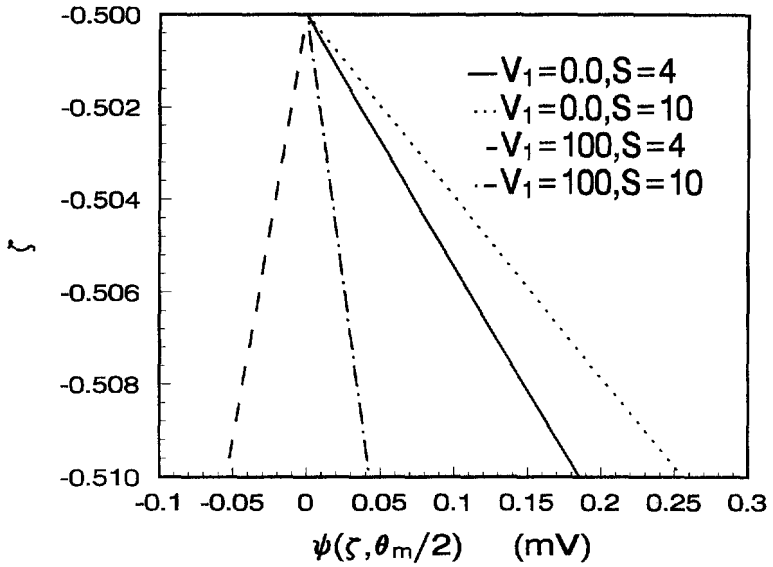

Fig. 8. The electric potential distribution in the sensor layer for Case 2 with $V_1 = 0$ and $V_1 = 100$ V.

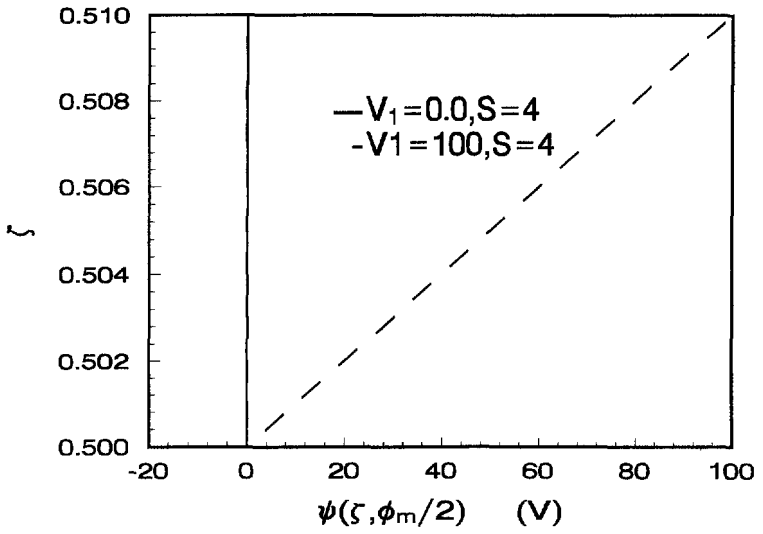

Fig. 9. The electric potential distribution in the actuator layer for Case 1 with $V_1 = 0$ and $V_1 = 100$ V.

REFERENCES

Bhaskar, K. and Varadan, T. K. (1993). Exact elasticity solution for laminated cylindrical anisotropic shells. *J. Appl. Mech.* **60,** 41–47.

Chandrashekhara, K. and Agarwal, A. N. (1993). Active vibration control of laminated composite plates using piezoelectric devices: a finite element approach. *J. Intell. Mater. Syst. Struct.* **4,** 496–508.

Crawley, E. F. and Lazarus, K. B. (1991). Induced strain actuation of isotropic and anisotropic plates. *AIAA J.* **29,** 944–951.

Crawley, E. F. and Luis de J. (1987). Use of piezoelectric actuators as elements of intelligent structures. *AIAA J.* **25,** 1373–1385.

Hwang, W. S. and Park, H. C. (1993). Finite element modeling of piezoelectric sensors and actuators. *AIAA J.* **31,** 930–937.

Ray, M. C., Bhattacharya, B. and Samanta, B. (1993a). Exact solution for static analysis of intelligent structures. *AIAA J.* **31,** 1684–1691.

Ray, M. C., Rao, K. M. and Samanta, B. (1993b). Exact solution for static analysis of an intelligent structure under cylindrical bending. *Comput. and Struct.* **47,** 1031–1042.

Ren, J. G. (1987). Exact solution for laminated cylindrical shells in cylindrical bending. *Comp. Sci. Tech.* **29,** 169–187.

Tzou, H. S. (1991). Distributed modal identification and vibration control of continua: theory and application. *J. Dyn. Syst. Measmt Cont.* **113,** 494–499.

Tzou, H. S. and Tseng, C. L. (1991). Distributed modal identification and vibration control of continua: piezoelectric element formulation and analysis. *J. Dyn. Syst. Measmt and Cont.* **113,** 500–505.

Wang, B. T. and Rogers, C. A. (1991). Laminated theory for spatially distributed induced strain actuators. *J. Comp. Mater.* **25,** 433–453.